# ON AN EFFICIENT AND ACCURATE METHOD TO INTEGRATE RESTRICTED THREE-BODY ORBITS

MARC A. MURISON
Department of Astronomy, University of Wisconsin–Madison, 475 North Charter Street, Madison, Wisconsin 53706
*Received 22 November 1988; revised 7 February 1989*

## ABSTRACT

Some workers currently use the Bulirsch–Stoer (BS) extrapolation method to solve ODEs associated with few-body dynamics, since it is fairly fast and apparently also accurate, while many others are currently unaware of the utility of the method. This work is a quantitative analysis of the advantages of the BS method, providing those already "in the know" with confidence in their BS integrators, and showing others that this method is certainly worth considering when working with small $N$ dynamical systems. Comparisons are made of different ways of using the method. The results, qualitatively suspected by many users, are quantitatively confirmed as follows: (1) The Bulirsch–Stoer extrapolation method is very fast and moderately accurate. (2) Regularization of the equations of motion stabilizes the error behavior of the method and is, of course, essential during close approaches. (3) When applicable, a manifold-correction algorithm, originally developed by Nacozy, reduces numerical errors to the limits of machine accuracy, and at the surprisingly small cost of approximately 0%–3% in cpu time. In addition, for the specific case of the restricted three-body problem, even a small eccentricity for the orbit of the primaries drastically affects the accuracy of integrations, whether regularized or not; the circular restricted problem integrates much more accurately, all else being equal.

## I. INTRODUCTION

The restricted three-body problem has in the past played an essential role in many different areas of dynamical astronomy, and indications are that this will continue (see, e.g., Valtonen 1988). The author has undertaken a study of the problem of satellite capture (Murison 1989; see also Huang and Innanen 1983), and the restricted three-body problem is a useful model with which to start. However, before beginning such a task, one must decide on specific numerical techniques and associated problems.

As the state of the art in computing becomes more advanced, larger numbers of integrations and longer durations are attempted. Thus, computational efficiency and accuracy are becoming ever more important, yet often they are not paid adequate attention. The author has noticed that a variety of methods are used by others (see Aarseth 1988 for a review), but that often little *quantitative* information is readily available regarding the accuracy and efficiency of some of these methods. This can and does lead to unwise choices for newcomers to small-body dynamics.

Recently, the Bulirsch–Stoer extrapolation method (Bulirsch and Stoer 1966) has caught the attention of the "cognoscenti," appearing to be fast and accurate. But just how accurate is it? Over what kinds of dynamical motions? How well can we *really* trust it? The current feeling is that it is probably a trustworthy method, at least in few-body dynamics—it is certainly pleasingly fast. This paper attempts to substantiate this feeling, using the restricted three-body problem as a test model.

The equations of motion of the massless particle of the restricted three-body problem are in two dimensions, and in a frame in which the primaries remain stationary (the "rotating–pulsating" frame),

$$x'' - 2y' = \frac{1}{1 + e_P \cos\theta}\frac{\partial\Omega}{\partial x},$$
$$y'' + 2x' = \frac{1}{1 + e_P \cos\theta}\frac{\partial\Omega}{\partial y}, \qquad (1)$$

where $\Omega = \frac{1}{2}(x^2 + y^2) + (1-\mu)/r_1 + \mu/r_2$ is an effective potential, $r_1$ and $r_2$ are the distances of the massless particle from the primaries $m_1$ and $m_2 < m_1$, $e_P$ is the eccentricity of the primary orbit, $\theta$ is the true anomaly of the primaries, and the mass ratio $\mu = m_2/(m_1 + m_2)$. The independent variable is $\theta$, and distances are scaled to the (nonconstant) primary separation. The more massive primary $m_1$ is located at $(x,y) = (-\mu,0)$, and the less massive primary is at $(1-\mu,0)$. The true anomaly $\theta$ is chosen as the independent variable instead of time, since the resulting equations (1) submit to regularization and are also simple and aesthetically pleasing. In addition, in many problems (for example, satellite capture) the rotating–pulsating frame of reference is much more intuitive and useful than the inertial frame.

In the circular case $e_P = 0$, an integral of the motion exists:

$$x'^2 + y'^2 - 2\Omega + C = 0. \qquad (2)$$

The nature of this particular dynamical problem requires high precision in the calculations, especially during long integrations which occur when studying satellite capture, implying that relatively large amounts of cpu time will be consumed. Later, we will be more specific about the kind of precision that is necessary. The problem is that a very small error can become greatly magnified as a calculation progresses, and soon the result can become meaningless—an expensive way to waste one's time. Unfortunately, speed and accuracy are usually at odds, and we must strike a compromise.

In this paper we consider numerical methods and requirements. First, the particular method with which one chooses to integrate the equations is shown to be very important. Next, we make use of the Jacobi constant to correct numerical truncation and roundoff errors in the circular restricted problem. This method can be applied to any problem in which constants of the motion exist. Finally, we incorporate regularization in the equations of motion. The effects of the various methods and techniques will be compared, using orbits in the circular restricted three-body (CRTB) and elliptic restricted three-body (ERTB) problems as test cases.

 0004-6256/89/051496-14$00.90 © 1989 Am. Astron. Soc. 1496

## II. BS INTEGRATION, REGULARIZATION, AND MANIFOLD CORRECTION

There are at least three ways to improve speed and accuracy in the integration of equations such as Eq. (1). First, use a fast and efficient algorithm. The Bulirsch–Stoer (BS) extrapolation method (see Press *et al.* 1986) is a very fast and efficient algorithm for solving ordinary differential equations like Eq. (1). It is also easy to code. Hénon (1969) was perhaps the first to use the BS method for the restricted problem, preferring it over Runge–Kutta. Second, take advantage of integrals of the motion for error checking and correction. Third, regularize the equations of motion. In the following, two-body regularization was incorporated (see, e.g., Stiefel and Scheifele 1970; Bettis and Szebehely 1971; Murison 1988).

### *a) Manifold Correction*

Nacozy (1971) found a clever way to use constants of the motion to monitor and correct errors in position and velocity. When an integral of the equations of motion exists, the orbit is confined to a surface in phase space. When a numerical error occurs, the motion jumps to a different surface, corresponding to a different orbit (Fig. 1). Nacozy's correction scheme uses Lagrange multipliers to find the least-squares shortest path back to the original manifold. Murison (1988) has applied this manifold correction to both the unregularized and regularized restricted three-body equations. Appendix B contains a summary of the technique.

One possible flaw in this approach is that the path taken back to the original manifold is not exactly the same one by which the system left it. So, even though the manifold on which the motion takes place remains constant to a very high degree of precision during a calculation, the actual orbit after each correction is not *exactly* the same one as before.

If, after a correction has been made, the resulting deviation on the manifold from the true orbit path is random, and if these random deviations are all small, then the calculated orbit will always closely follow the true orbit ("true orbit" = "orbit calculated with infinite precision"). However, if the resulting deviations are systematic, then the calculated orbit will eventually diverge from the true orbit. This could arise if the errors themselves are systematic. Then, taking the shortest path back to the manifold will produce a systematic component to the errors, and sooner or later the calculated and true orbits will diverge significantly.

As usual in situations like this, one depends on the fact that the corrections are exceedingly small so that, even over the course of a long integration, the difference between the orbit one calculates and the true orbit is negligible. In the circular restricted three-body (CRTB) test orbits used here, corrections were made whenever the difference between the current and initial Jacobi constant was nonzero. In practice, this means that $C$ was kept constant to a precision of roughly $10^{-16}$. This is 6–10 orders of magnitude more precise than previous CRTB calculations (see, for example, Huang and Innanen 1983; Carusi *et al.* 1983; Heppenheimer and Porco 1977; Horedt 1976; Byl and Ovenden 1975; Heppenheimer 1975; Benest 1971, 1974; and Hunter 1967a,b).

A more rigorous statement of this argument is as follows. Let $\Gamma$ be the set of points defined by the true orbit, and let $\Gamma'$ be the set of points defined by the computed orbit. $\Gamma$ lies on the manifold $M$ defined by the constraint, Eq. (2). That is,

$$\Gamma = \{\Gamma(\theta) \mid \theta \in \mathrm{R}^1\} \subset M,$$

where the function $\Gamma(\theta)$ is the infinitely precise solution of Eqs. (1). Define a small neighborhood $U$ of $\Gamma$. Furthermore, define the set of points $\gamma$,

$$\gamma = \{\gamma(\theta,\psi) \mid (\theta,\psi) \in \mathrm{R}^1 \times \mathrm{R}^1\} \subset U,$$

where $\psi$ is a winding number. Let $\gamma$ be such that for any given $\theta$ (and $\psi$) the distance between $\gamma(\theta,\psi)$ and $\Gamma(\theta)$

$$\|\gamma(\theta,\psi) - \Gamma(\theta)\| = \eta,$$

where $\eta$ is a small nonnegative constant. That is, $\gamma$ is a cylindrical tube of fixed radius $\eta$ centered on $\Gamma$ and contained in $U$. Now, if the condition

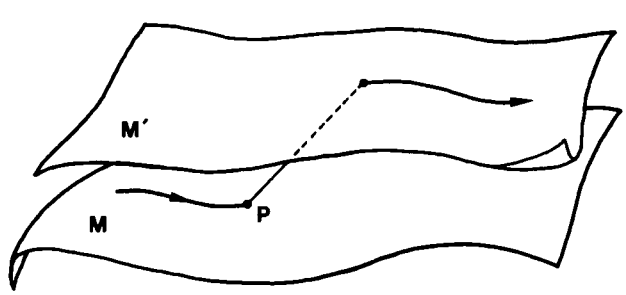


FIG. 1. Original manifold $M$. A numerical error occurs at $P$, sending the orbit path to a new manifold $M'$.

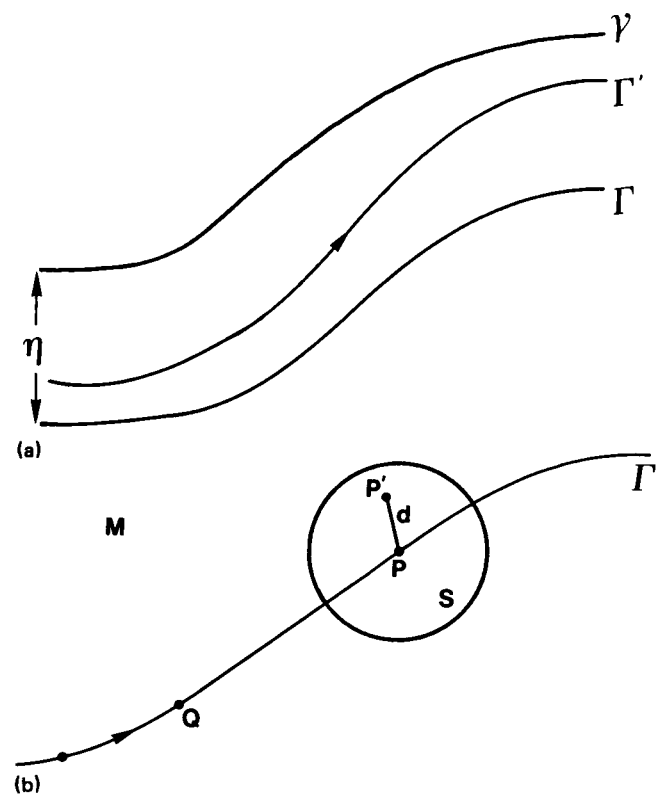


FIG. 2. (a) Condition for sufficient accuracy: the computed orbit $\Gamma'$ is always closer to the true orbit $\Gamma$ than some fictitious set of points $\gamma$, which is a fixed distance $\eta$ from $\Gamma$. The set $\gamma$ is a cylindrical tube surrounding $\Gamma$; for clarity, only the upper intersection with the page is shown. (b) The computed orbit $\Gamma'$, which initially coincides with the true orbit $\Gamma$, is represented in a piecewise continuous fashion by dots at each step in $\theta$. The plane of the page represents the manifold $M$. An error occurs at $Q$, sending the next point (not shown) of $\Gamma'$ off of $M$. At the next step, manifold correction returns $\Gamma'$ to $M$ at the point $P'$, which lies at a distance $d$ from $P$, the point to which $\Gamma'$ would have gone had there been no error. The distance $d$ is less than the radius $\zeta$ of a circle on $M$ (see the text). The area bounded by the circle represents the set $S$.

$$\|\Gamma'(\theta) - \Gamma(\theta)\| < \eta, \quad \forall\theta\in\mathbf{R}^1 \tag{3}$$

is satisfied, then the computed orbit $\Gamma' \subset U$ for all $\theta$. In other words, if Eq. (3) is true, then $\Gamma'$ is constrained to accurately follow $\Gamma$ at all times (see Fig. 2(a)).

Now, when a numerical error occurs, $\Gamma'$ leaves $M$. At the next step, the manifold-correction (MC) algorithm makes an appropriate correction to bring $\Gamma'$ back to $M$. Let $P \subset M$ be the point on $M$ to which $\Gamma'$ would have gone if no error had occurred, and let $P' \subset M$ be the actual point to which the MC algorithm returns $\Gamma'$ (Fig. 2(b)). The flaw mentioned above has the consequence that, in general, $P' \neq P$.

Let the distance on $M$ between $P'$ and $P$ be called $d$. Assume that $d$ is never larger than some number $\zeta < \eta$. That is,

$$d \leqslant \zeta < \eta, \quad \forall\theta\in\mathbf{R}^1.$$

Let $S \subset M$ be the set of points contained by the circle on $M$ centered on $P$ and of radius $\zeta$ (refer to Fig. 2(b)). Then, if the calculated return point $P'$ is randomly distributed on $S$, condition (3) holds, and $\Gamma' \subset U$ for all $\theta$. If, however, $P'$ is not randomly distributed on $S$, then it is likely that $\Gamma'$ will drift out of $U$ in a finite number of integration steps.

In practice, $\zeta$ appears to be extremely small, especially with a correction occurring at nearly every step. So, even if $P'$ is not randomly distributed on $S$, any drift across $U$ is so slow that for all *practical* purposes $\Gamma' = \Gamma$. A further study to determine the size of $\zeta$, the average size of $d$, and the distribution of $P'$ on $S$ would be interesting, but it is not attempted here.

### *b) Regularization*

One can also make coordinate transformations in the equations of motion in order to find a representation that will integrate more quickly and/or accurately. In typical problems, the major source of error is close approaches. This is because of the $1/r$ terms in the gravitational potential; a small error becomes magnified for small $r$. If we make a $1/r$ transformation of the coordinates and time (known as local, or Levi–Civita, regularization—see Szebehely 1967; Stiefel and Scheifele 1970; Bettis and Szebehely 1971; Murison 1988), then the $r^{-3}$ singularity in the force terms disappears. Appendix A contains a brief summary of the specific equations used here for the restricted three-body problem.

When these transformations are incorporated, calculations speed up by a factor of roughly 1.5–3, depending on the particular orbit. Even more important, the *character* of error behavior is greatly improved over the "real" coordinate calculations.

Fortunately, it is also possible to incorporate the manifold-correction scheme of Nacozy into the CRTB regularized equations. The details of this are shown in Appendix B (see also Murison 1988).

### *c) Test Orbits*

To illustrate the usefulness of these techniques, the orbit shown in Fig. 3 was integrated several different ways. This

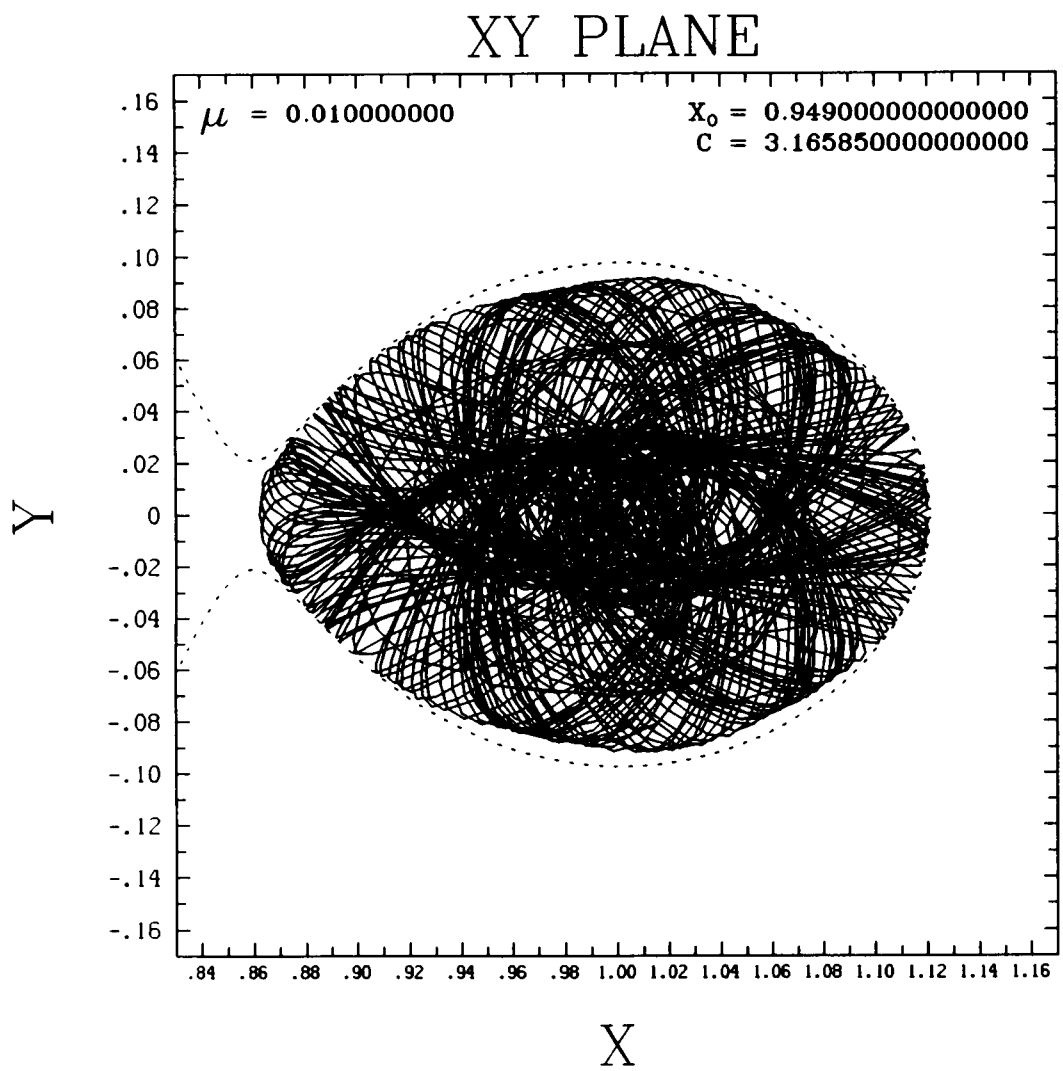


FIG. 3. Test orbit used for the calculations of Figs. 4–6.

orbit is difficult in the sense that it has many close approaches to $m_2$. The integration continued for 40 orbital periods of the primaries. In each case except the first, an effort was made to keep the amount of machine work the same.

During the integration, the error in the Jacobi constant $\Delta C$ was monitored. A measure of the accumulated error is also useful in characterizing the accuracy of an orbit. Thus, the quantity C defined by

$$C = \int |\Delta C| \, dt$$

was also monitored.

The curve labeled "RK" in Fig. 4 shows the error in $C$ during an integration that used an efficient, fourth-order Runge–Kutta (RK) method with variable step size. Notice the steady increase of error with time. The cpu time needed by a VAX 11/780 was 2522 s. The value of C was $2.13 \times 10^{-10}$. The curve labeled "BS" shows the same calculation, this time using the BS method. Discrete jumps are caused by close approaches, and are often larger than those in the RK case. However, the cpu time required was more than a factor of 10 less (242 s). The value of C was $3.22 \times 10^{-12}$. Thus, the BS method is both more accurate and much faster than RK.

Figure 5 shows the effect of manifold correction (MC). The BS method was used again, and whenever an error in $C$ occurred MC was used at the next step. Notice the drastic collapse of the errors. What would have been a large jump in $C$ is reduced to a narrow spike. Yet there was no increased cost in cpu time (241 s)! Here, C dropped over two orders of magnitude, to a value of $2.23 \times 10^{-14}$.

To illustrate the effect of regularization, Fig. 6 shows the result of using the BS method without manifold correction but with regularized equations of motion (the curve labeled "BS + R"). Note that *the vertical scale has been magnified by a factor of 1000.* The errors are extremely small, compared to the previous figures. This is a result of keeping the amount of machine effort about the same (cpu time was 235 s). Notice that the character of the error behavior has also improved: instead of relatively large jumps, as in the BS curve of Fig. 4, the errors are a combination of spikelike and steady drift behavior. C was, in this case, $2.82 \times 10^{-15}$.

Finally, the curve labeled "BS + MC + R" shows the result of combining the BS method, regularization, and manifold correction. The cpu time required was 236 s. Again, the cost of MC was negligible. The errors have been reduced to effectively nothing, with a net savings of cpu time, compared to the BS method alone. Notice that the maximum error that occurred is only $\Delta C = 3.4 \times 10^{-15}$, compared to $2.1 \times 10^{-11}$ for BS alone. Also, C was a very tiny $1.57 \times 10^{-17}$.

Thus, we conclude that the BS method of integration is very fast, and, when combined with regularization and especially manifold correction, extremely accurate. Regularization significantly stabilizes the method. We also note the importance of regularization and the small cost of manifold

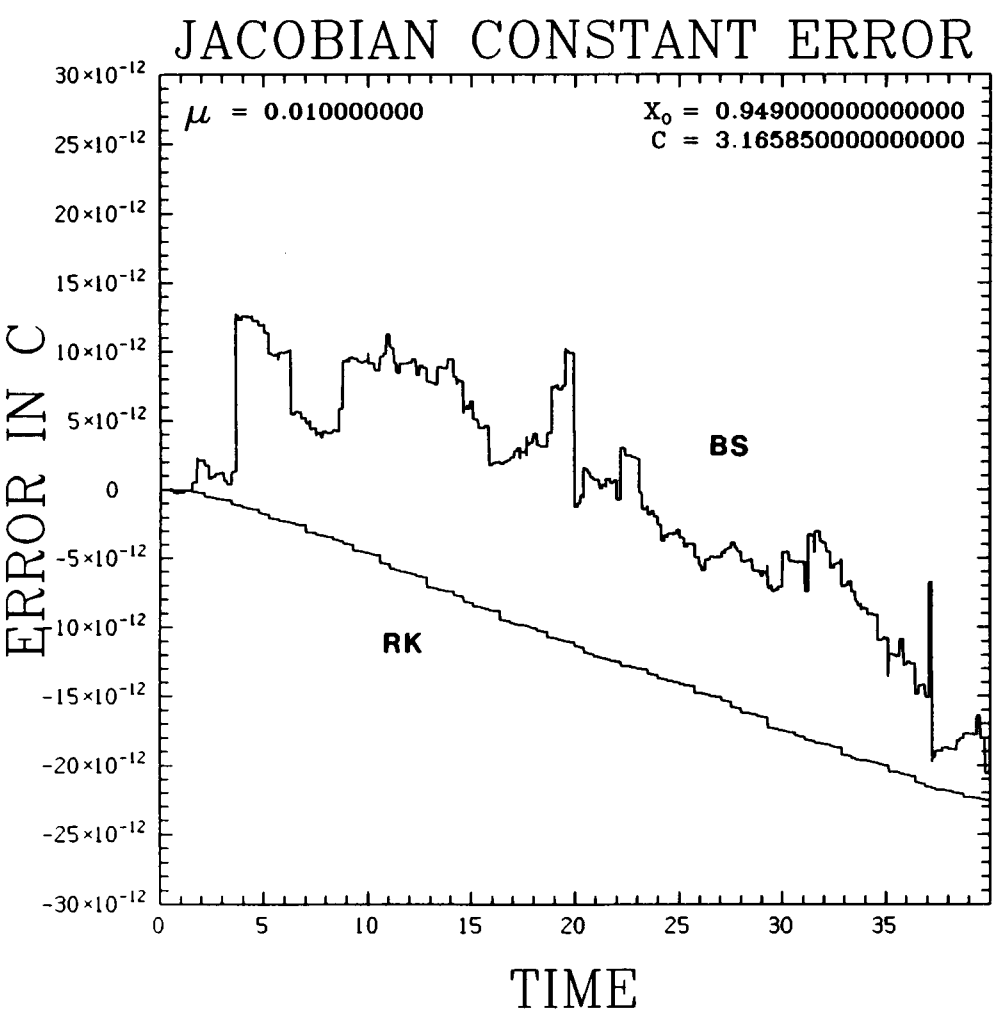


FIG. 4. Error in the Jacobi constant $C$ vs time in units of the primary orbital period. BS = Bulirsch–Stoer, RK = fourth-order Runge–Kutta. The RK calculations took ten times more cpu time than the BS calculations.

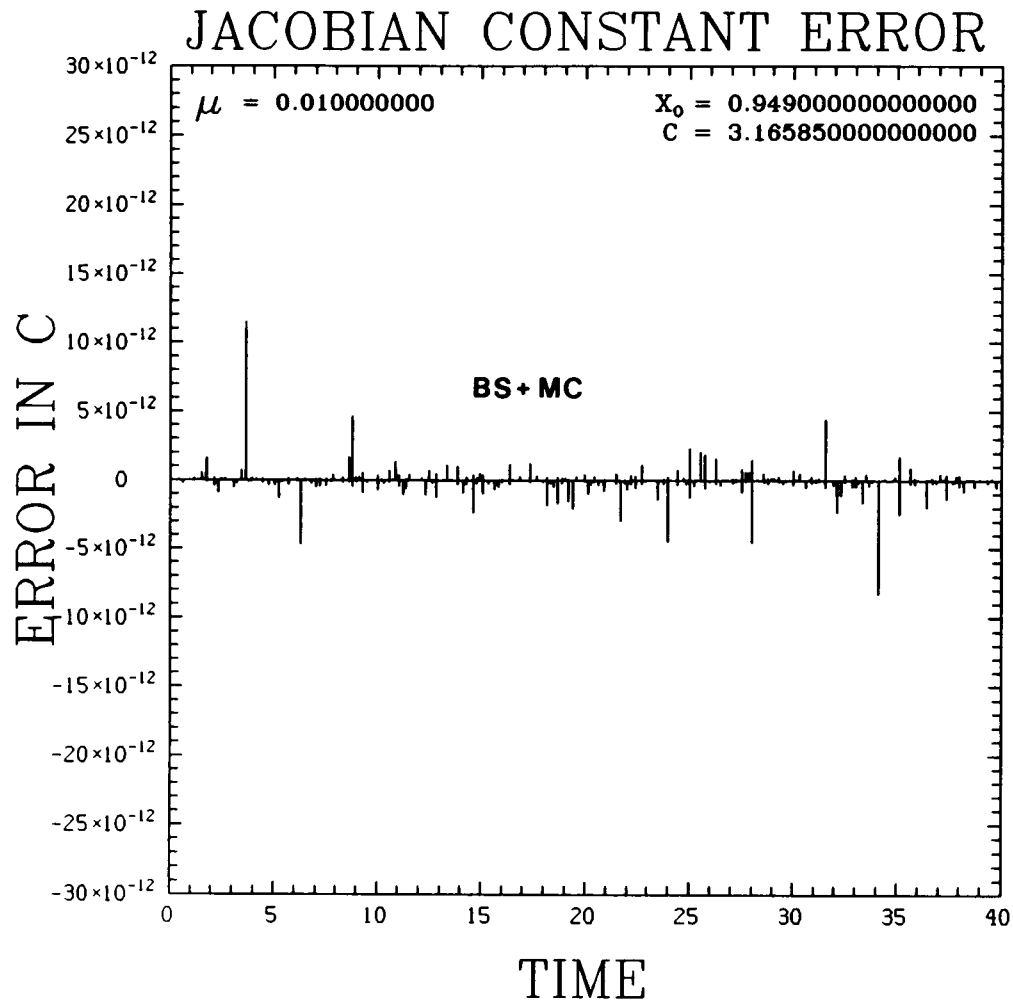


FIG. 5. Error in the Jacobi constant versus time. Bulirsch–Stoer, with manifold correction. Note drastic reduction of errors (compare with Fig. 4).

correction (in general, the author has noticed the cost to vary between approximately 0% and 3% in cpu time). Table I summarizes the results. Notice that the combination of manifold correction and regularization has decreased C by more than five orders of magnitude. Regularization alone decreased C by over three orders of magnitude. The maximum error has been decreased by over four orders of magnitude.

### III. BACKWARDS-INTEGRATION CHECK

In order to further check the accuracy of the BS integrator, and also BS combined with regularization, four different orbits were integrated forward for one hundred revolutions of the primaries and then backward to $T = 0$ again, once with unregularized equations of motion and then again with regularized equations. The start and end values of the coordinates were then compared. A forward-integration time of one hundred primary revolutions is not exceedingly large, but it is long enough to obtain a quantitative illustration of the kinds of errors and under what conditions they occur.

The four test orbits consist of the "easy" orbit of Fig. 7(a), which has no close approaches and zero eccentricity for the primary motion ($e_P = 0$); an orbit very similar to the one of Fig. 7(a), but with a finite eccentricity for the primary motion of $e_P = 0.0482$ (that of the Jupiter–Sun system); the orbit of Fig. 7(b), which has many close approaches, but the primary eccentricity is zero; and the orbit of Fig. 7(c), similar to that of Fig. 7(b), except that now $e_P = 0.0482$ again. These will be referred to as cases 1–4, respectively. Figure 7(d) shows the distance from $m_2$ as a function of time for the orbit of Fig. 7(c) (case 4). The many close approaches make this orbit, and the one of Fig. 7(b), difficult tests of the integration method, especially for unregularized equations.

Most integrators with adjustable step size have an accuracy parameter which determines the relative accuracy of an integration. We shall call this parameter $\epsilon$. One would expect that for small $\epsilon$ an integration would be accurate and believable, and that as $\epsilon$ is increased, eventually a point is reached where the errors are so large as to make the integration meaningless—the global character of the orbit is altered. Each of cases 1–4 were repeated for many different values of $\epsilon$; for our specific example of BS integrator (essentially that of Press *et al.* 1986), $\epsilon$ ranged from $10^{-9}$ to $10^{-15}$.

A good indicator of whether, after a backwards integration, the character of an orbit has changed or not is $\Delta x$, the error in the $x$ position of the orbit ($\Delta y$ would probably work just as well). Other possible indicators include the error in energy $\Delta E$ and the error in phase-space position, $\Delta r_p = \sqrt{(\Delta x)^2 + (\Delta y)^2 + (\Delta v_x)^2 + (\Delta v_y)^2}$. Figure 8(a) shows the log of $\Delta E$ plotted against the log of $\Delta x$, for the orbit of case 1. Figure 8(b) shows the log of $\Delta r_p$ plotted against the log of $\Delta x$. We see that the correlation between $\Delta E$ and $\Delta x$ is very good. Thus, the error in energy is a good indicator of whether or not the character of an orbit trajectory is changing. The correlation between $\Delta r_p$ and $\Delta x$ appears to be a bit more ragged.

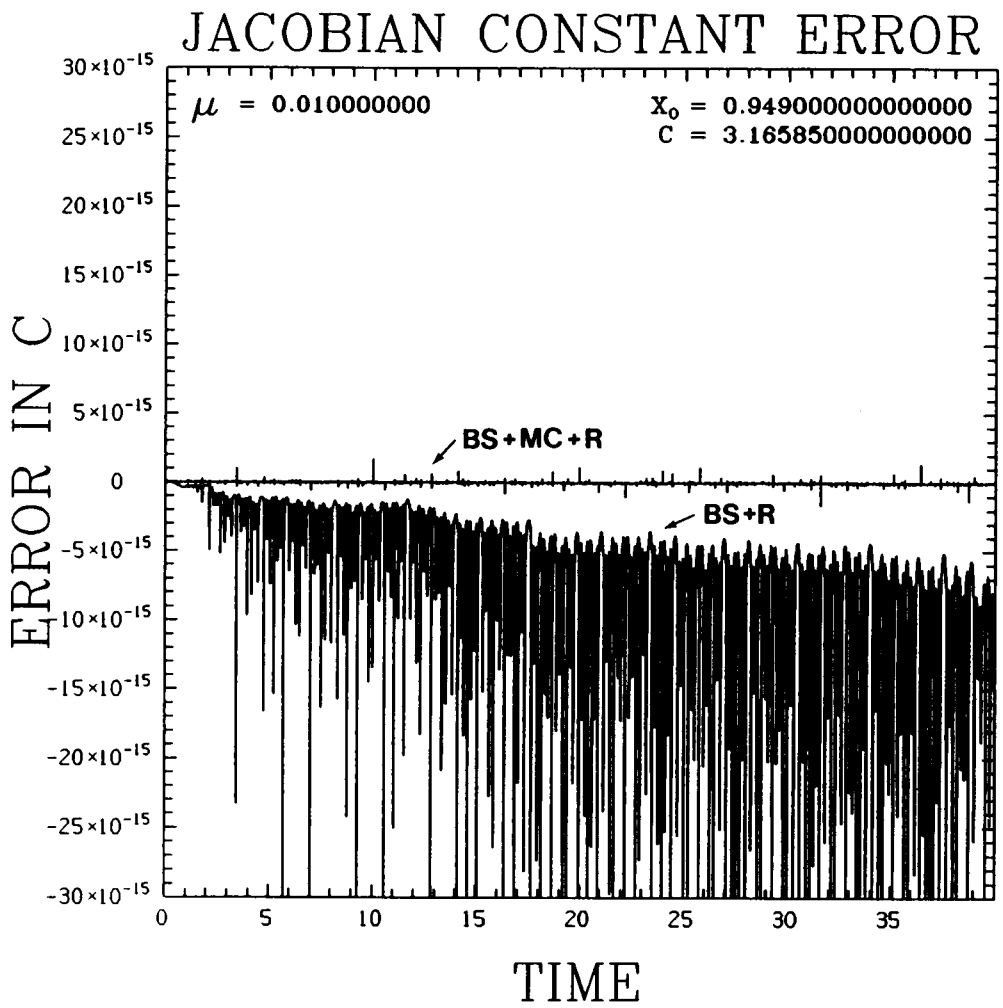


FIG. 6. Error in Jacobi constant versus time. Curve labeled BS + R is Bulirsch–Stoer and regularized equations. BS + MC + R is a combination of Bulirsch–Stoer, manifold correction, and regularization. Notice the factor of 1000 change in scale.

The results of the backward integrations are shown in Figs. 9–12. In Fig. 9 is case 1, the "easy" orbit with $e_P = 0$, first with unregularized equations of motion (Fig. 9(a)), and then with regularized equations (Fig. 9(b)). Plotted is the error in $x$ versus forward-integration time in units of the primary period. Each trace corresponds to a different value of the accuracy parameter $\epsilon$, which varied in uniform steps of log $\epsilon$. Figures 10–12 are similar, for cases 2–4, respectively.

There are several effects to note. First, we look at those due to regularization. As can be seen, for the "easy" orbits (cases 1 and 2), regularization improves the accuracy of the integration, as measured by $\Delta x$, by a factor of roughly 30–100. For the "difficult" orbits (cases 3 and 4), regularization improves the accuracy by a factor of approximately 1000. Note that for larger values of $\epsilon$, the regularized integrations are of relatively poor accuracy for cases 3 and 4. The limit of highly accurate integrations appears to be approximately $\epsilon \simeq 10^{-11.4}$ when regularization is used. For $\epsilon$ greater than this cutoff, the errors in $x$ position are (relatively) large and erratic when compared to integrations for which $\epsilon$ is smaller than the cutoff. This is seen in Figs. 11(b) and 12(b). When there are no close approaches (Figs. 9(b) and 10(b)), the regularized integrations are well behaved.

TABLE I. Summary of Figs. 4–6.

| Case | $\int \lvert\Delta C\rvert\, dt$ | $\lvert\Delta C\rvert_{max}$ | CPU (sec) |
|---|---|---|---|
| RK | $2.13\times10^{-10}$ | $2.22\times10^{-11}$ | 2522 |
| BS | $3.22\times10^{-12}$ | $2.06\times10^{-11}$ | 242 |
| BS+MC | $2.23\times10^{-14}$ | $1.15\times10^{-11}$ | 241 |
| BS+R | $2.82\times10^{-15}$ | $1.68\times10^{-13}$ | 235 |
| BS+MC+R | $1.57\times10^{-17}$ | $3.44\times10^{-15}$ | 236 |

In addition to providing higher accuracy, regularization can also reduce the cpu time required. For cases 3 and 4, the cpu time needed to perform the unregularized calculations ranged from 50% to 70% more than that needed for the regularized calculations. On the other hand, for cases 1 and 2, the regularized calculations took 12%–18% longer. Therefore, cpu savings results during close approaches. In every case though, the regularized calculation was much more accurate.

It should be pointed out that in none of the cases did $\Delta x$ exceed $3\times10^{-3}$. Thus, the BS integration method appears to be quite good in general—at least for integration times of one hundred primary periods or less for the restricted problem with close approaches.

Also very significant are the effects due to eccentricity of the primary orbit. When regularization is not used, the $e_P = 0$ orbits (cases 1 and 3) are more accurate than the $e_P \neq 0$ orbits (cases 2 and 4) by factors of roughly $10^5$. When

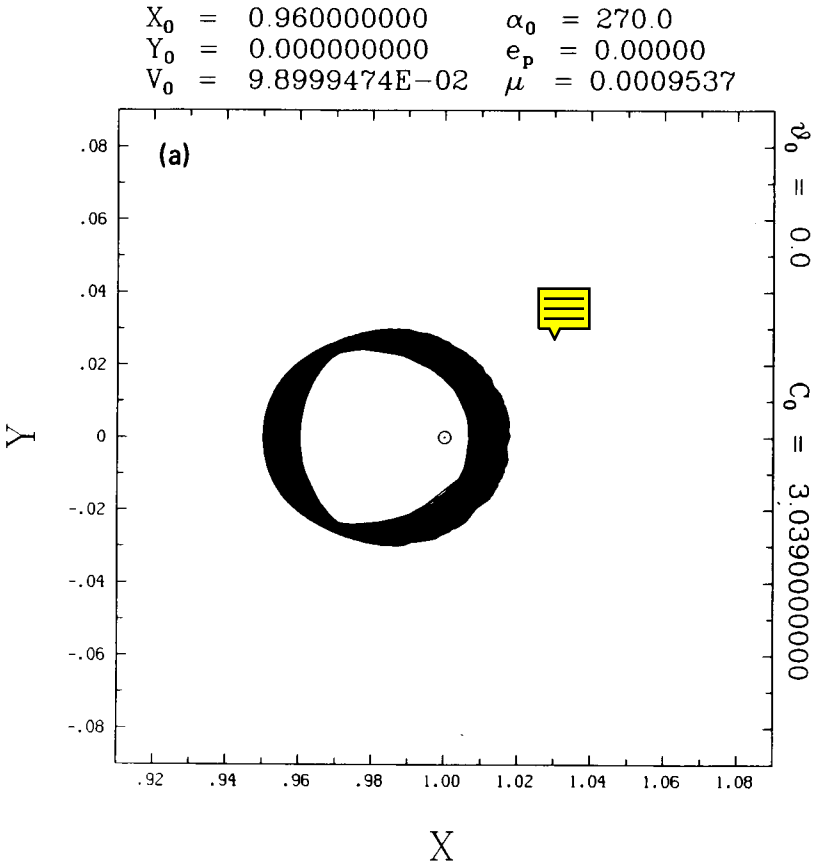


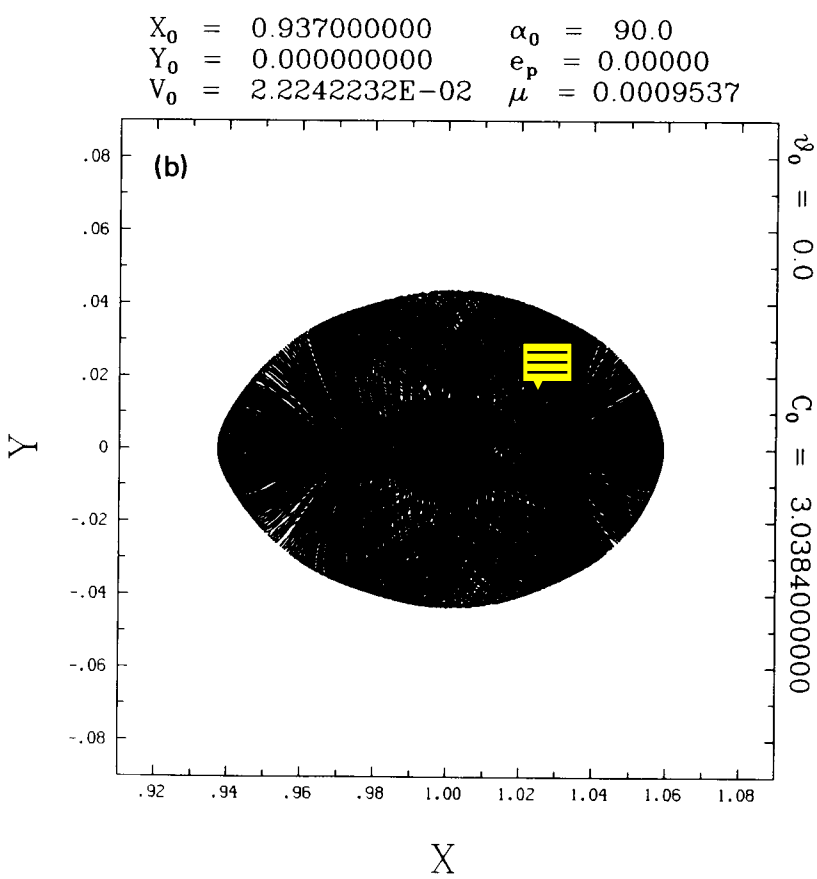


FIG. 7. (a) The backwards-integration test orbits for case 1; (b) case 3; and (c) case 4. (d) The distance from $m_2$ as a function of primary orbital periods, for the orbit of case 4.

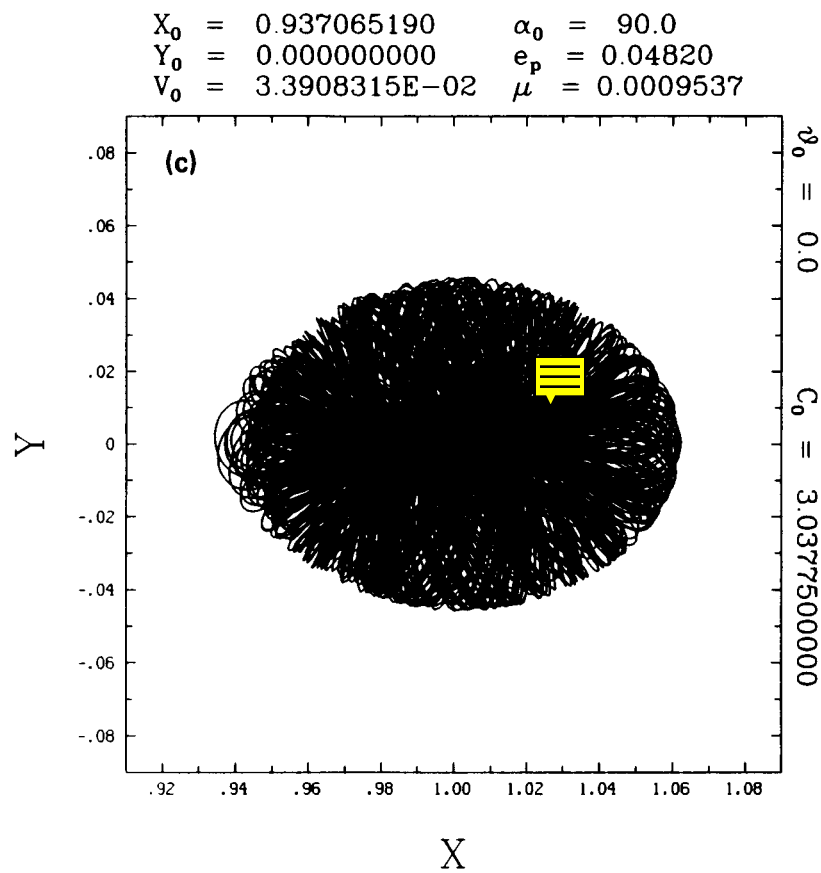


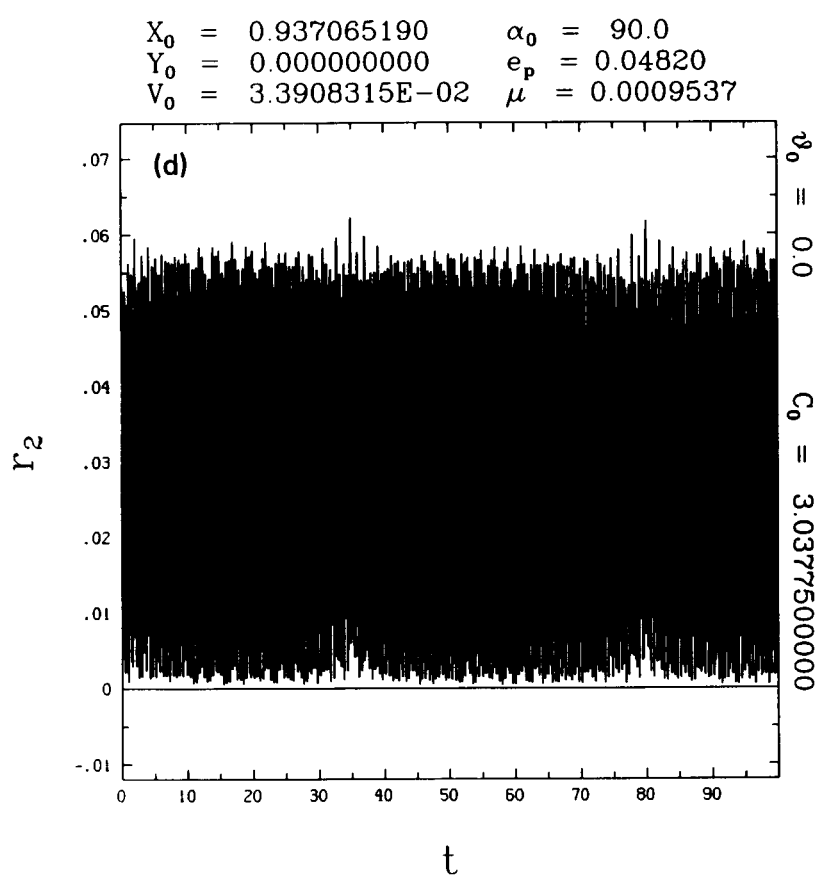


FIG. 7. (continued)

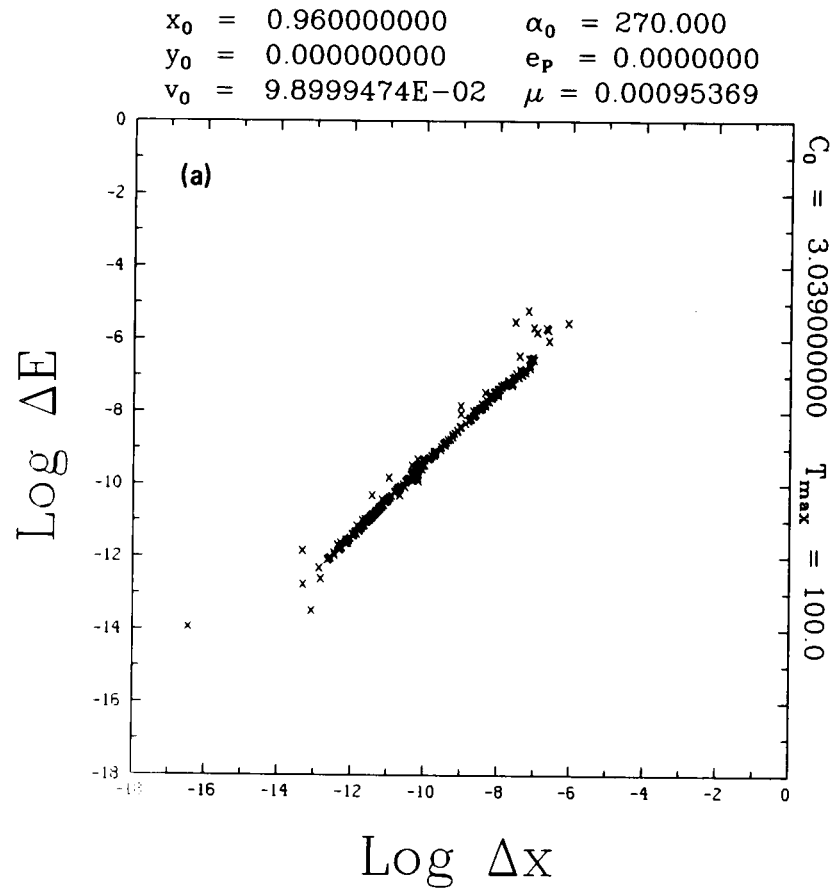


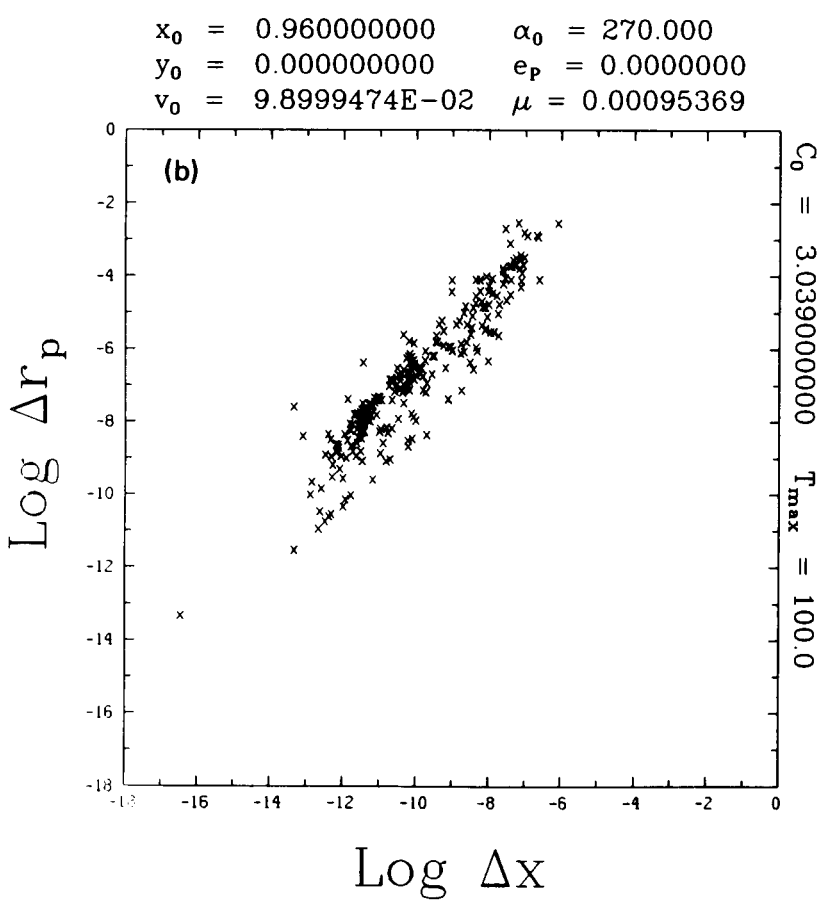


FIG. 8. (a) log of $\Delta E$ plotted against the log of $\Delta x$, for the orbit of case 1. (b) the log of $\Delta r_p$ plotted against the log of $\Delta x$.

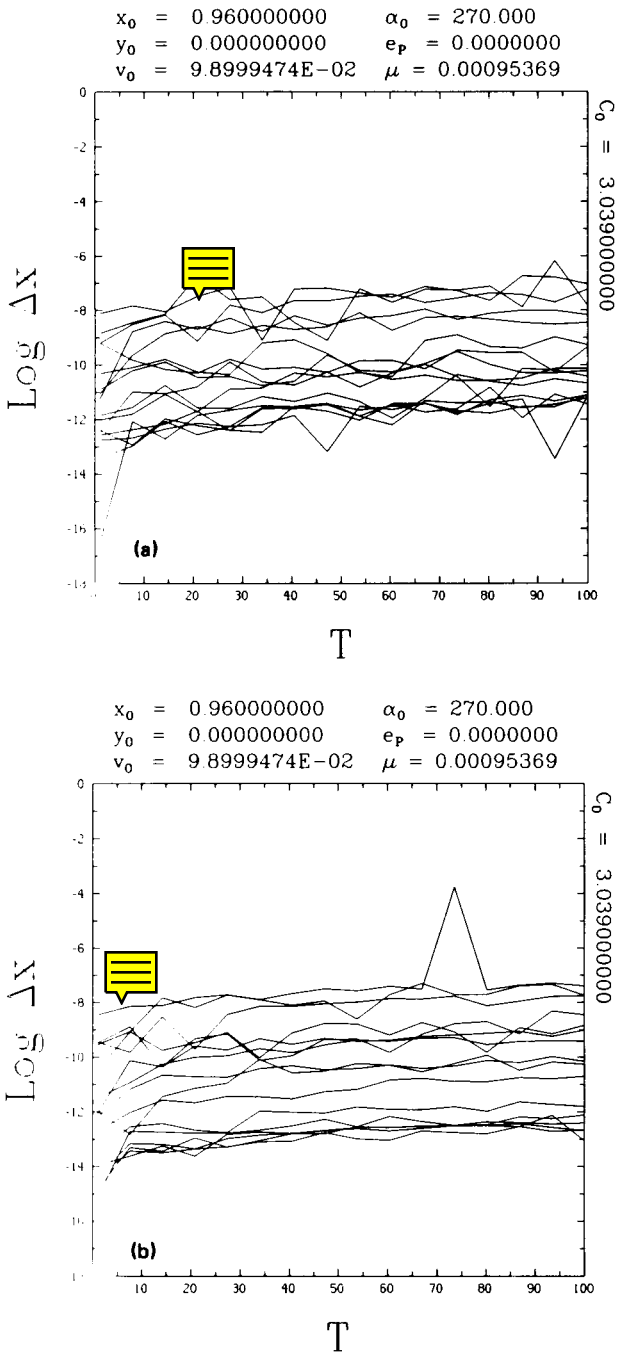


FIG. 9. Error in $x$ as a function of forward-integration time, for several values of the accuracy parameter $\epsilon$ ranging from $10^{-9}$ to $10^{-15}$. The orbit is that of Fig. 7(a) (case 1). (a) Unregularized equations and (b) regularized equations.

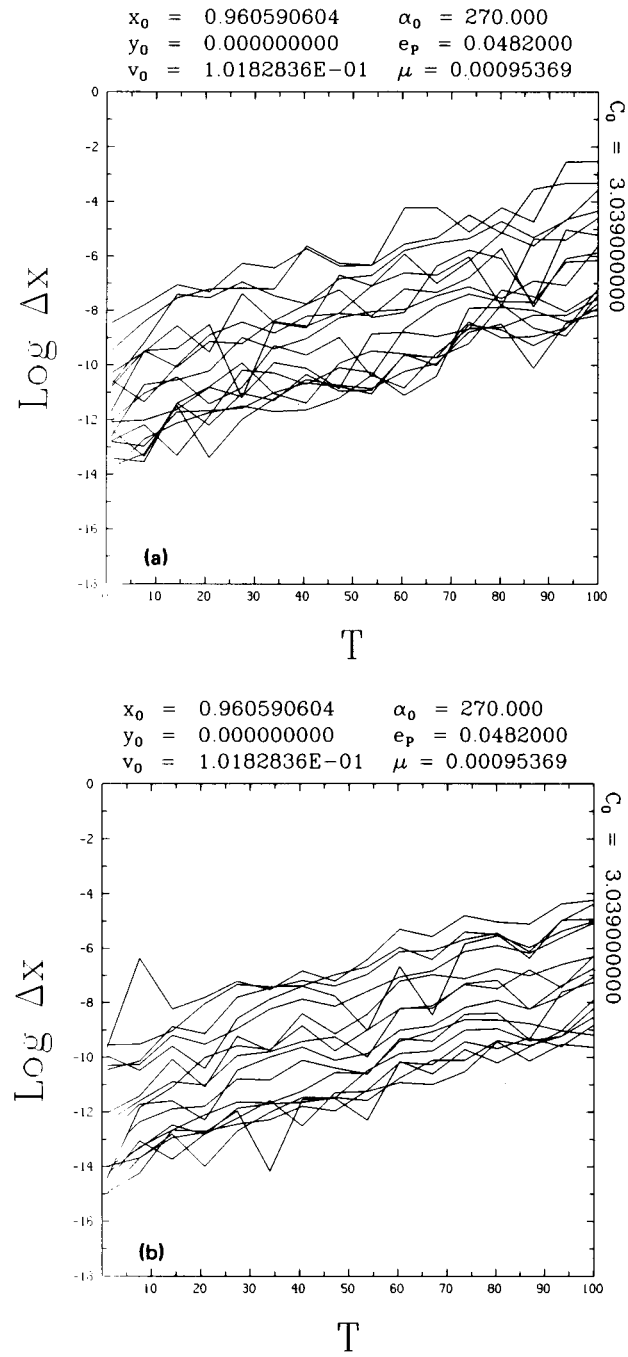


FIG. 10. Same as in Fig. 9, except for the orbit of case 2 (similar to case 1, but with nonzero primary eccentricity).

regularization is incorporated, the $e_P = 0$ orbits are more accurate by a factor of $\sim 10^1$ for the difficult orbit and $\sim 10^3$ for the easy orbit. Thus, even a small eccentricity such as $e_P = 0.048$, corresponding to the Jupiter–Sun system, drastically affects the accuracy of the integrations.

In addition, one can see that $\Delta x$ is increasing much more rapidly with increasing forward-integration time for the $e_P \neq 0$ orbits than for the $e_P = 0$ orbits. We have, very roughly,

$$\log \Delta x \simeq \frac{1}{100} T + \text{const.}, \quad e_P = 0,$$

$$\log \Delta x \simeq \frac{5}{100} T + \text{const.}, \quad e_P = 0.048.$$

The slopes seem to be approximately independent of whether or not regularization was used. The eccentricity of the primaries is certainly the major effect.

It is tempting to use the slopes of the traces in Figs. 9–12 to predict upper bounds for forward-integration time. For example, based on an extrapolation of Fig. 11(b) for $\epsilon = 10^{-14}$, we would expect $\Delta x$ to be roughly $10^{-3}$ after a forward and then backward integration of about 1100 primary periods. Yet, an actual calculation yields $\Delta x = 10^{-11.8}$

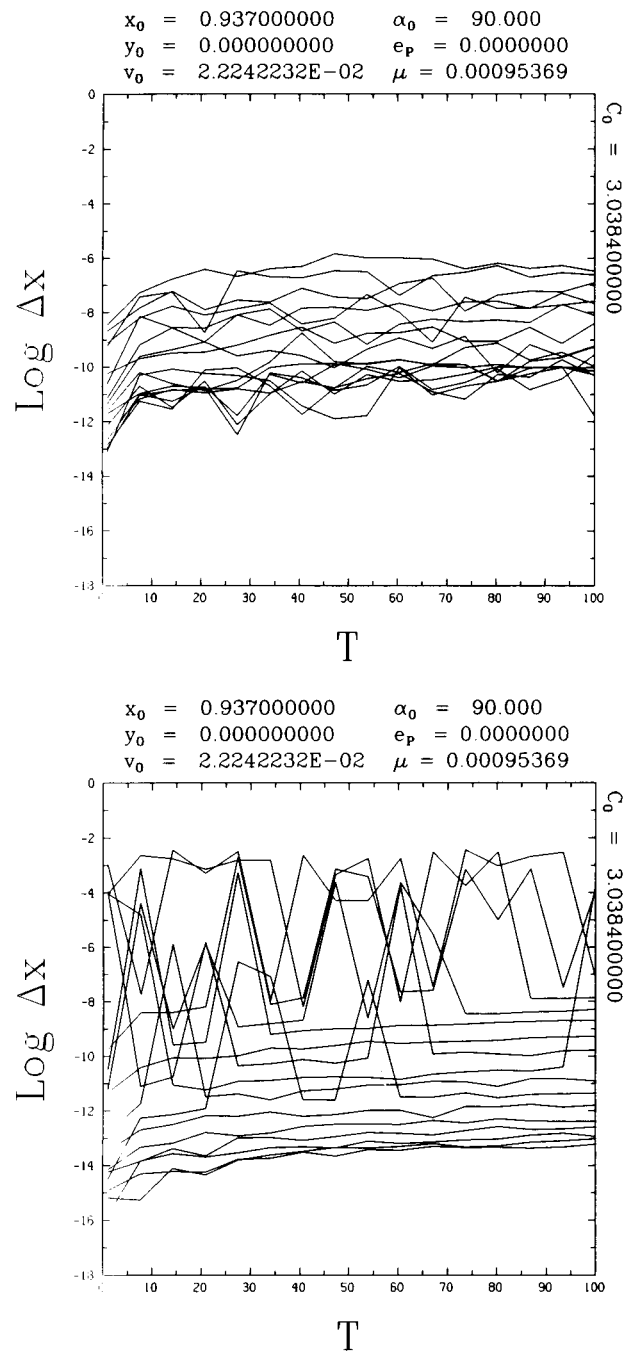


FIG. 11. Same as in Fig. 9, except for the orbit of case 3.

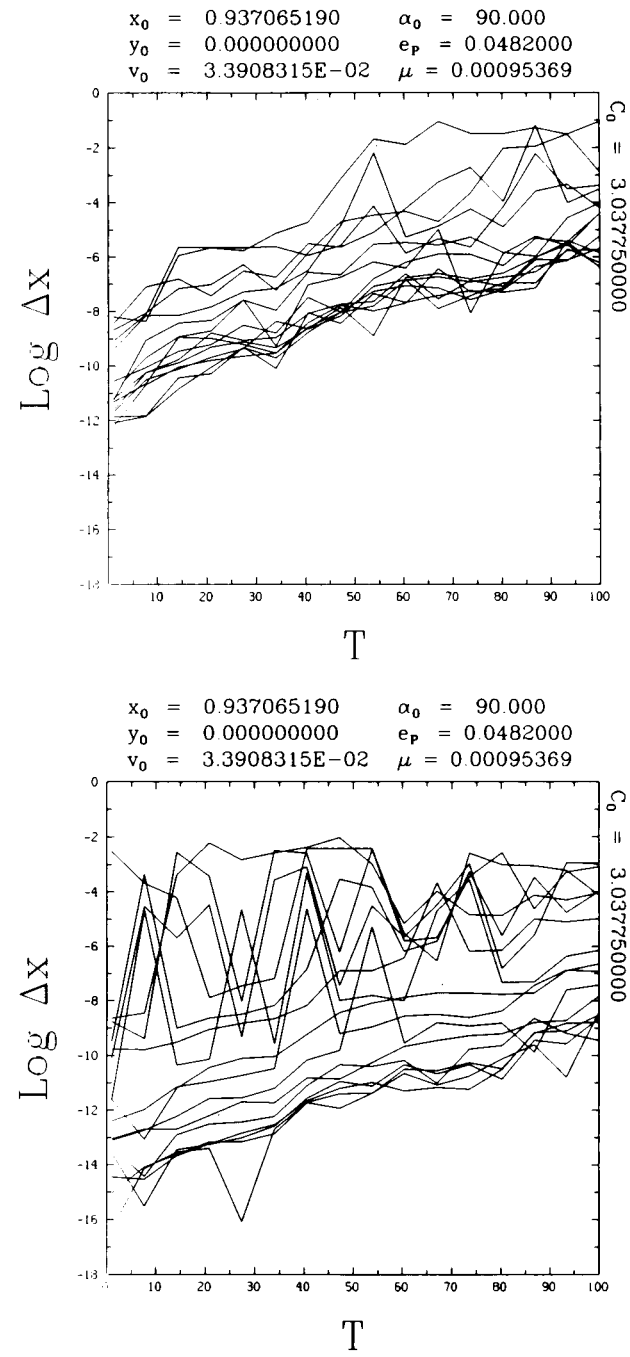


FIG. 12. Same as in Fig. 9, except for the orbit of case 4.

instead. To take another example, from Fig. 12(b) we would expect $\Delta x$ to be $10^{-3}$ after a forward and then backward integration of about 230 primary periods, with $\epsilon = 10^{-14}$. Yet, after an integration 1400 primary periods forward and then back, $\Delta x$ was still only $10^{-3.2}$. Thus, it seems that predictions of maximum integration time based on Figs. 9–12 are not at all reliable, and calculations are indeed trustworthy for much longer times.

## V. CONCLUSIONS

We see that the BS extrapolation method is indeed very fast, and by itself also fairly accurate. Errors are on the same order of magnitude as those produced by the ever-popular Runge–Kutta, but integrations proceed about an order of magnitude faster. Regularization of the equations of motion, besides having the well-known properties of making close approaches possible to calculate and reducing machine effort, also significantly stabilizes the BS method's error behavior. The manifold-correction scheme of Nacozy (1971) can reduce the errors to effectively zero (the limit being set by the word size of the machine), and at the surprisingly small cost in cpu time of 0%–3%, depending on the orbit. Unfortunately, its implementation depends on the existence of at least one integral of the motion. Finally, in the specific case of the restricted three-body problem, we found that nonzero eccentricity of the primaries significantly reduces the accuracy of integrations, compared to the circular case.

The BS method currently is used by several workers, for whom it seems to be a good method, at least for small $N$ dynamical systems. Here the author hopes to have shown that the method is indeed as good *quantitatively* as it seems qualitatively, and that current users of the method can feel reassured. The author also hopes that this discussion will convince others who are currently using or plan to use other methods that they may profit considerably by considering BS and Nacozy's manifold correction (if it can be applied). These methods are also attractive in that they are easy to code and implement.

The author thanks Arthur D. Code, Marc Balcells, and Barbara A. Whitney for encouragement, criticisms, and support. He also thanks the anonymous referee for some very constructive criticism. Extensive allocation of computing resources was granted by the Midwestern Astronomical Data Reduction and Analysis Facility (MADRAF); many thanks go to Christopher M. Anderson for such considerations. This work is part of the author's Ph.D. research, and was supported in part by NASA contracts nos. NAS5-26777 and 65B-580912.

## APPENDIX A: REGULARIZATION

### *a) The Equation of Motion*

The equations of motion (1) can be transformed via the Kustaanheimo–Stiefel transformation (Kustaanheimo and Stiefel 1965; also Stiefel and Scheifele 1970; Bettis and Szebehely 1971) into regularized form.

The transformation is as follows. Introduce a new set of coordinates (dependent variables) $\boldsymbol{\omega} = (\omega_1,\omega_2)^T$ and a new "time" (independent variable) $\tau$, such that

$$\boldsymbol{\chi} = \mathbf{W}(\boldsymbol{\omega}) ,$$
$$\frac{d\theta}{d\tau} = \alpha(\boldsymbol{\omega}) , \tag{A1}$$

where $\boldsymbol{\chi} = (x+\mu,y)^T$ or $\boldsymbol{\chi} = (x-1+\mu,y)^T$, depending on whether $r_1$ or $r_2$, respectively, is the regularized quantity, $\theta$ is the true anomaly of the primaries, and $\mathbf{W}$ and $\alpha$ are

$$W_1 = \omega_1^2 - \omega_2^2 ,$$
$$W_2 = 2\omega_1\omega_2 ,$$
$$\alpha(\boldsymbol{\omega}) = \chi \equiv W(\boldsymbol{\omega}) .$$

Sundman (1912) used this form for $\alpha$, and it came to be known as Sundman's transformation for the independent variable. It can be shown that this type of regularization can be performed in two or four dimensions, but not three (Stiefel and Scheifele 1970). Thus, $\mathbf{W}$ is four dimensional for the case of three spatial dimensions (see Stiefel and Scheifele (1970) and Bettis and Szebehely (1971)).

#### *1) Elliptic case*

The regularized form of Eqs. (1) can then be written (see Murison 1988)

$$\boldsymbol{\omega}'' - \frac{1}{2}H\boldsymbol{\omega} = \frac{1}{2}W\mathbf{G} ,$$
$$H' = 2\boldsymbol{\omega}'\cdot\mathbf{G} - \frac{df}{d\theta} , \tag{A2}$$
$$\theta' = W ,$$

where $H$ is an auxiliary variable related to the energy, and a prime denotes differentiation with respect to $\tau$. Also, it is convenient that $W = \boldsymbol{\omega}\cdot\boldsymbol{\omega} = \omega_1^2 + \omega_2^2$. The function $f(\theta)$ is

$$f(\theta) = \begin{Bmatrix} \dfrac{1-\mu}{1+e_p\cos\theta} , & \boldsymbol{\chi} = \mathbf{r}_1 \\ \dfrac{\mu}{1+e_p\cos\theta} , & \boldsymbol{\chi} = \mathbf{r}_2 \end{Bmatrix} .$$

The vector $\mathbf{G}$ is

$$G_1 = 4\omega_2' + h(\theta)k_1 ,$$
$$G_2 = -4\omega_1' + h(\theta)k_2 , \tag{A3}$$

where the components of $\mathbf{k}$ are

$$k_1 = \omega_1\{(W-1)[1-(\mu/r_2^3)] + 1 - \mu\} ,$$
$$k_2 = \omega_2\{(W+1)[1-(\mu/r_2^3)] - (1-\mu)\} , \tag{A4}$$

if $r_1$ is being regularized, or

$$k_1 = \omega_1\{(W+1)[1-(1-\mu)/r_1^3] - \mu\} ,$$
$$k_2 = \omega_2\{(W-1)[1-(1-\mu)/r_1^3] + \mu\} , \tag{A5}$$

if $r_2$ is being regularized. The function $h(\theta)$ is

$$h(\theta) = \frac{1}{1+e_p\cos\theta} .$$

#### *2) Circular case*

When the eccentricity of the primaries is zero (the circular restricted case), the planar regularized equations of motion simplify to

$$\boldsymbol{\omega}'' - \tfrac{1}{2}(U - \tfrac{1}{2}C)\boldsymbol{\omega} = \tfrac{1}{2}W\mathbf{G} ,$$
$$\theta' = W , \tag{A6}$$

where $C$ is the Jacobi constant (Eq. (2)), $U$ is

$$U = \begin{cases} \tfrac{1}{2}(x^2+y^2) + (\mu/r_2) , & \chi = r_1 \\ \tfrac{1}{2}(x^2+y^2) + (1-\mu)/r_1 , & \chi = r_2 \end{cases} \tag{A7}$$

and the components of $\mathbf{G}$ are now

$$G_1 = 4\omega_2' + k_1 ,$$
$$G_2 = -4\omega_1' + k_2 .$$

### *b) Initialization of the Regularized Variables*

At the beginning of an orbit calculation, the initial conditions will usually be specified in "normal"-space coordinates. Thus, we need to be able to set the regularization variable values when given the normal-space values. That is, we need the transformation whose inverse is Eqs. (A1). In two dimensions, we have

$$\chi_1 = \begin{Bmatrix} x+\mu , & \boldsymbol{\chi} = \mathbf{r}_1 \\ x-1+\mu , & \boldsymbol{\chi} = \mathbf{r}_2 \end{Bmatrix} = \omega_1^2 - \omega_2^2 ,$$
$$\chi_2 = y = 2\omega_1\omega_2 , \tag{A8}$$

and the first derivatives,

$$\chi_1' = \frac{d\chi_1}{d\theta} = \frac{1}{W}\frac{d\chi_1}{d\tau} = \frac{2}{W}(\omega_1\omega_1' - \omega_2\omega_2'),$$
$$\chi_2' = \frac{2}{W}(\omega_1\omega_2' + \omega_2\omega_1') . \tag{A9}$$

If we add and subtract Eqs. (A8) to and from $\boldsymbol{\omega}\cdot\boldsymbol{\omega} = W = \chi$, we find

$$\boldsymbol{\omega}\cdot\boldsymbol{\omega}+\chi_1=2\omega_1^2\,,$$
$$\boldsymbol{\omega}\cdot\boldsymbol{\omega}-\chi_1=2\omega_2^2\,.$$

Thus, it must be true that

$$\omega_1=\pm\sqrt{\frac{\chi+\chi_1}{2}}\,,\quad \omega_2=\pm\sqrt{\frac{\chi-\chi_1}{2}}\,.$$

The question now arises of which signs for $\omega_1$ and $\omega_2$ do we choose. The problem stems from the fact that the regularization space is double valued. That is, the four quadrants of the $x$–$y$ plane are mapped into eight regions in the $\omega_1$–$\omega_2$ plane (Szebehely 1967). Because of this duplicity, we are free to choose. When $y>0$, then, from Eq. (A8), $\omega_1$ and $\omega_2$ must both be of the same sign. We will arbitrarily choose the positive. When $y<0$, then $\omega_1$ and $\omega_2$ are of opposite sign. We will arbitrarily choose the negative for $\omega_1$ and the positive for $\omega_2$. Thus, we have the starting value convention

$$\omega_1=\begin{cases}+\sqrt{\dfrac{\chi+\chi_1}{2}}\,, & \chi_2>0\\[2ex] -\sqrt{\dfrac{\chi+\chi_1}{2}}\,, & \chi_2<0,\end{cases}$$

$$\omega_2=+\sqrt{\frac{\chi-\chi_1}{2}}\,.$$

Now we determine the initial regularized velocities $\omega_1'$ and $\omega_2'$. From Eq. (A9) we write

$$\tfrac{1}{2}W\chi_1'=\omega_1\omega_1'-\omega_2\omega_2'\,,$$
$$\tfrac{1}{2}W\chi_2'=\omega_1\omega_2'+\omega_2\omega_1'\,.$$

Use these to construct the combinations

$$\tfrac{1}{2}W(\omega_1\chi_1'+\omega_2\chi_2')=(\omega_1^2+\omega_2^2)\omega_1'=W\omega_1'\,,$$
$$\tfrac{1}{2}W(\omega_1\chi_2'-\omega_2\chi_1')=(\omega_1^2+\omega_2^2)\omega_2'=W\omega_2'\,.$$

Thus, once we have determined the initial values of $\omega_1$ and $\omega_2$, the initial values of $\omega_1'$ and $\omega_2'$ can be determined from

$$\omega_1'=\tfrac{1}{2}(\omega_1\chi_1'+\omega_2\chi_2')\,,$$
$$\omega_2'=\tfrac{1}{2}(\omega_1\chi_2'-\omega_2\chi_1')\,.$$

Finally, we assign the initial value of $H$ as follows,

$$H=\frac{1}{2}\boldsymbol{\chi}'\cdot\boldsymbol{\chi}'-\frac{f(\theta)}{W}\,,$$

where $\boldsymbol{\chi}'=d\boldsymbol{\chi}/d\theta$.

For a more thorough discussion, see Murison (1988).

## APPENDIX B: REGULARIZED MANIFOLD CORRECTION

### *a) Manifold Correction*

In this Appendix, we briefly state a result of Nacozy (1971) and apply it to the circular restricted three-body (CRTB) problem, which has an integral of the motion (the Jacobi constant), for both the unregularized and the regularized forms.

At a particular instant in time, let the computed state vector be $\boldsymbol{\xi}$ and the corresponding ideal (i.e., infinite precision) state vector be $\mathbf{x}$, where

$$\boldsymbol{\xi}\equiv\begin{pmatrix}\xi\\ \xi'\\ \eta\\ \eta'\\ \zeta\\ \zeta'\end{pmatrix}\quad\text{and}\quad \mathbf{x}\equiv\begin{pmatrix}x\\ x'\\ y\\ y'\\ z\\ z'\end{pmatrix}.$$

$\boldsymbol{\xi}$ contains numerical errors and must be corrected to get back to the ideal, error-free state vector $\mathbf{x}$. Let the correction vector be $\boldsymbol{\epsilon}$, such that

$$\boldsymbol{\xi}+\boldsymbol{\epsilon}=\mathbf{x}\,.$$

Define a constraint function $\phi(\mathbf{x})$ to be the energy constant of the system. In the case of the circular restricted three-body problem, we use the Jacobi constant relation (2),

$$\phi(\mathbf{x})\equiv\mathbf{v}^2-2\Omega+C=0\,, \tag{B1}$$

where $v^2\equiv x'^2+y'^2$, Then, from Nacozy (1971), we can compute the components of the correction vector according to

$$\epsilon_i=\left[-\phi(\boldsymbol{\xi})\Big/\left|\frac{\partial\phi}{\partial\boldsymbol{\xi}}\right|^2\right]\frac{\partial\phi}{\partial\xi_i}\,, \tag{B2}$$

where for notational convenience the derivatives are interpreted in the following sense:

$$\frac{\partial\phi}{\partial\boldsymbol{\xi}}\equiv\left.\frac{\partial\phi}{\partial\mathbf{x}}\right|_{\boldsymbol{\xi}}$$

and

$$\frac{\partial\phi}{\partial\xi_i}\equiv\left.\frac{\partial\phi}{\partial x_i}\right|_{\xi_i}\,.$$

Differentiation of $\phi$ is with respect to the $x_i$ evaluated at $\xi_i$. It is *not* to be interpreted as the derivative with respect to the $\xi_i$.

Equation (B2) gives the components $\epsilon_i$, which, when added to the computed state vector $\boldsymbol{\xi}$, give

$$\phi(\mathbf{x})=0$$

to order $|\boldsymbol{\epsilon}|^2$. In addition, the $\epsilon_i$ have been chosen so that the length of the correction vector squared is minimized.

Geometrically, the vector $\boldsymbol{\epsilon}$ is normal to a hyperplane that is approximately tangent to the five-dimensional hypersurface, defined by Eq. (B1), at the point $\mathbf{x}$. Equation (B1) is the actual hypersurface, to which

$$\phi(\boldsymbol{\xi})+\boldsymbol{\epsilon}\cdot\frac{\partial\phi}{\partial\boldsymbol{\xi}}\simeq\phi(\mathbf{x})$$

is a first-order approximation.

For reference, the derivatives of $\phi$, as given by Eq. (B1), are

$$\frac{\partial\phi}{\partial x}=-2x+2\left[\frac{1-\mu}{r_1^3}(x+\mu)+\frac{\mu}{r_2^3}(x-1+\mu)\right],$$
$$\frac{\partial\phi}{\partial y}=-2y\left(1-\frac{1-\mu}{r_1^3}-\frac{\mu}{r_2^3}\right),$$
$$\frac{\partial\phi}{\partial x'}=2x'\,,$$
$$\frac{\partial\phi}{\partial y'}=2y'\,.$$

### *b)Manifold Correction with Regularization*

We can also use manifold correction with the CRTB equations when they are in regularized form (see Appendix A).

The Jacobi constant relation is, in normal space,

$$v^2 - 2\Omega + C = 0\,, \tag{B3}$$

where

$$\Omega = \frac{1}{2}(x^2 + y^2) + \frac{1-\mu}{r_1} + \frac{\mu}{r_2}\,.$$

Since Eq. (B3) is to be our constraint function, we need to write it in the regularized variables. The "velocity" can be written

$$v^2 = 4\,\frac{\boldsymbol{\omega}' \cdot \boldsymbol{\omega}'}{W}\,,$$

while the effective potential can be written

$$\Omega = U + \frac{1}{W}\begin{cases} 1-\mu\,, & \chi = r_1 \\ \mu\,, & \chi = r_2 \end{cases},$$

where $U$ is given by (A7). So Eq. (B3) becomes

$$4\,\frac{\boldsymbol{\omega}' \cdot \boldsymbol{\omega}'}{W} - 2\left[U + \frac{1}{W}\begin{pmatrix} 1-\mu \\ \mu \end{pmatrix}\right] + C = 0\,.$$

Thus, we write the constraint function (B1) in the form

$$\phi = 2\boldsymbol{\omega}' \cdot \boldsymbol{\omega}' - W\left(U - \frac{1}{2}C\right) - \begin{pmatrix} 1-\mu \\ \mu \end{pmatrix} = 0\,. \tag{B4}$$

In order to use Eq. (B2) to form the correction vector $\boldsymbol{\epsilon}$, we need the derivatives of Eq. (B4). Making use of the fact that $x = \omega_1^2 - \omega_2^2$ and $y = 2\omega_1\omega_2$, we calculate the derivatives of $\phi$ and arrive at the result

$$\frac{\partial\phi}{\partial\boldsymbol{\omega}} = -2(H\boldsymbol{\omega} + W\mathbf{k})\,,$$

$$\frac{\partial\phi}{\partial\boldsymbol{\omega}'} = 4\boldsymbol{\omega}'\,, \tag{B5}$$

where $H = U - \frac{1}{2}C$ is the auxiliary variable of Appendix A, and the vector $\mathbf{k}$ is given by Eqs. (A4) or (A5).

A prescription for applying manifold correction to the regularized CRTB equations of motion is as follows:

(1) Transform $\boldsymbol{\omega}$ to $x$ and $y$ and calculate $U$ according to Eq. (A7).

(2) Calculate the constraint function $\phi$ from Eq. (B4).

(3) Calculate the components of $\mathbf{k}$ from Eqs. (A4) or (A5).

(4) Calculate the derivatives of $\phi$ according to Eq. (B5).

(5) Form the correction vector $\boldsymbol{\epsilon}$ according to Eq. (B2).

(6) Add the corrections to $\boldsymbol{\omega}$ and $\boldsymbol{\omega}'$.

(7) If the equations of motion are in the general ERTB form (Eq. (A2)) instead of the specific CRTB form (Eq. (A6)), then $H$ will have to be recalculated, using the new (corrected) state vector, from $H = U - \frac{1}{2}C$.

## REFERENCES


Aarseth, S. J. (1988). In *The Few Body Problem*, edited by M. J. Valtonen (Kluwer, Dordrecht), p. 287.

Benest, D. (1971). Astron. Astrophys. **13**, 157.

Benest, D. (1974). Astron. Astrophys. **32**, 39.

Bettis, D. G., and Szebehely, V. (1971). Astrophys. Space Sci. **14**, 133.

Byl, J., and Ovenden, M. W. (1975). Mon. Not. R. Astron. Soc. **173**, 579.

Carusi, A., Perozzi, E., and Valsecchi, G. B. (1983). In *Dynamical Trapping and Evolution in the Solar System*, edited by V. V. Markellos and Y. Kozai (Reidel, New York).

Hénon, M. (1969). Astron. Astrophys. **1**, 223.

Heppenheimer, T. A. (1975). Icarus **24** 172.

Heppenheimer, T. A., and Porco, C. (1977). Icarus **30**, 385.

Horedt, G. P. (1976). Astron. J. **81**, 675.

Huang, T.-Y., and Innanen, K. A. (1983). Astron. J. **88**, 1537.

Hunter, R. B. (1967a). Mon. Not. R. Astron. Soc. **136**, 245.

Hunter, R. B. (1967b). Mon. Not. R. Astron. Soc. **136**, 267.

Kustaanheimo, P., and Stiefel, E. (1965). J. Math. **218**, 204.

Murison, M. A. (1988). Ph.D. thesis, University of Wisconsin–Madison.

Murison, M. A. (1989). In preparation.

Nacozy, P. E. (1971). Astrophys. Space Sci. **14**, 40.

Press, W. H., Flannery, B. P., Teukolsky, S. A., and Vetterling, W. T. (1986). *Numerical Recipes: The Art of Scientific Computing* (Cambridge University, Cambridge).

Stiefel, E., and Scheifele, G. (1970). *Linear and Regular Celestial Mechanics* (Springer, New York).

Sundman, K. F. (1912). Acta. Math. **36**, 105.

Szebehely, V. (1967). *Theory of Orbits* (Academic, New York).

Valtonen, M. J. (1988). *The Few Body Problem*, edited by M. J. Valtonen (Kluwer, Dordrecht).